

AAS 10-266

A VARIATIONAL METHOD FOR THE PROPAGATION OF SPACECRAFT RELATIVE MOTION

Giulio Baù,^{*} Claudio Bombardelli,[†] Jesús Peláez,[‡]
Enrico Lorenzini[§] and Alessandro Francesconi[¶]

A new formulation of the spacecraft relative motion for a generic orbit is presented based on the orbital propagation method proposed by Peláez et al. in 2006 [1]. Two models have been developed. In the first model the method is applied to each spacecraft using a time synchronization of the system dynamical states. In the second model we employ a local orbital reference frame with a linearization of gravitational terms, apply the method to the formation center of mass and propagate the relative dynamics with respect to the center of mass reference orbit. The models are compared in terms of computational speed for the case of a bounded triangular formation.

INTRODUCTION

The study of relative motion between satellites is of great importance in space technology. Usually the relative motion of the generic spacecraft, called “chaser”, is expressed in an orbital frame moving with a reference spacecraft, called “target”. The first model of relative motion was developed by Hill [2] in his work on the lunar theory. Clohessy and Wiltshire (CW) [3] adapted Hill’s equations to the problem of satellite rendezvous in the 1960s. The Hill-CW equations of relative motion were derived assuming that the distance between the target and the chaser is small compared with the radius of the target circular orbit. These equations can be analytically integrated if the motion is supposed to be unperturbed, and the solutions are used to obtain a rough prediction of the relative dynamics for short time spans. Lawden [4] was the first to formulate and determine the analytical solutions of the linearized equations of relative motion valid for elliptical orbits. Many other authors have obtained solutions for this case, the most known are Tschauner and Hempel [5], who, like Lawden, use the true anomaly as the independent variable, and de Vries [6], Melton [7], Yamanaka Ankersen [8] and Broucke [9], who use time as the independent variable.

Analytical solutions to the problem of relative motion provide a tool for the preliminary design of a formation flight. Besides, they are preferred to numerical integrators in applications where an onboard computer is used to calculate the relative position respect to an other spacecraft. However, the big drawback of analytical solutions is that they lose accuracy with time, and for long-term predictions numerical algorithms are required.

In 2006 Peláez et al. [1] formulated a special perturbation method that propagates the orbit of a material particle affected by any kind of perturbations with a very fast and accurate numerical integration. The variation of parameters technique is applied to a particular set of elements, which are chosen as the integrals of the unperturbed motion. The special perturbation method is free of singularities related to small inclination and/or eccentricity.

In this article, we resume Peláez method [1] proposing an alternative derivation of the variational equations by means of the Poisson’s formulation. We present relations between the new integrals of the motion introduced in [1] and the classical integrals of the two-body problem. Then, we use this propagator in the problem

^{*}Ph.D. Candidate, University of Padova, Centro Interdipartimentale Studi e Attività Spaziali, Padova, 35131, Italy; also Visiting Student, Technical University of Madrid, ETSI Aeronáuticos, Plaza Cardenal Cisneros 3, Madrid 28040, Spain.

[†]Research Fellow, Technical University of Madrid, ETSI Aeronáuticos, Plaza Cardenal Cisneros 3, Madrid 28040, Spain.

[‡]Professor, Technical University of Madrid, ETSI Aeronáuticos, Plaza Cardenal Cisneros 3, Madrid 28040, Spain.

[§]Professor, University of Padova, Faculty of Engineering, Padova, 35131, Italy.

[¶]Research Fellow, University of Padova, Centro Interdipartimentale Studi e Attività Spaziali, Padova, 35131, Italy.

of determining the relative motion between the spacecraft of a formation flight respect to the formation center of mass. Two approaches are proposed. In the first, the method is applied to each spacecraft, and the relative dynamic states respect to the center of mass are calculated after the integration by operating a difference between two absolute dynamic states. In the second approach, the method is applied only to the center of mass, which is chosen as the reference target point, and the equations of relative motion are linearized and expressed in an inertial reference frame. An example of a bounded triangular formation is used to compare the models in terms of computational speed.

ORBITAL PROPAGATION OF ONE POINT MASS

The special perturbation method of Peláez et al. [1] is a fast and accurate orbital propagator of one point mass flying around a primary body of attraction. The method applies the variation of parameters technique to a new set of integrals of the two-body motion after introducing an independent variable different from time. We explain the meaning of the new independent variable and the new integrals, and we apply the Poisson's approach to derive the variational equations.

Two-body problem

Let us consider a particle of mass m moving inside the sphere of influence of a primary. We introduce an inertial frame $\mathcal{I} = \{O; \mathbf{i}_X, \mathbf{i}_Y, \mathbf{i}_Z\}$ with the origin O placed at the primary center of mass. Let \mathbf{r} be the vector that defines the particle position P respect to O at time t , as shown in Fig. (1). The Newton's Second Law applied to the mass m appears in the form

$$m\ddot{\mathbf{r}} = -m\frac{\mu}{r^3}\mathbf{r} + \mathbf{F}_p(\mathbf{r}, \dot{\mathbf{r}}, t) \quad (1)$$

where μ is the gravitational parameter of the primary and \mathbf{F}_p is the perturbation force vector. The *two-body problem* is to find the time evolution of \mathbf{r} for $t > t_0$ by solving Eq. (1) given the initial conditions

$$\begin{aligned} \mathbf{r}(t_0) &= \mathbf{r}_0 \\ \dot{\mathbf{r}}(t_0) &= \dot{\mathbf{r}}_0. \end{aligned}$$

We will call the two-body problem *unperturbed* and *perturbed* when respectively $\mathbf{F}_p = \mathbf{0}$ and $\mathbf{F}_p \neq \mathbf{0}$.

The unperturbed two-body problem is analytically solvable and the solution is a *keplerian* orbit characterized by six independent *integrals*. Five integrals specify the shape and the inertial orientation of the orbit, for instance the specific angular momentum vector

$$\mathbf{h} = h \mathbf{u}_h = \mathbf{r} \times \dot{\mathbf{r}} \quad (2)$$

and the eccentricity vector

$$\mathbf{e} = e \mathbf{u}_e = \frac{\dot{\mathbf{r}} \times \mathbf{h}}{\mu} - \frac{\mathbf{r}}{r} \quad (3)$$

where h , e and \mathbf{u}_h , \mathbf{u}_e are the magnitudes and the directions of \mathbf{h} , \mathbf{e} . The sixth integral sets the particle position P_0 in the orbit at time t_0 , for instance the initial true anomaly

$$\vartheta_0 = \vartheta - \int_{t_0}^t \frac{h}{r^2} dt \quad (4)$$

where ϑ can be computed as

$$\vartheta = \cos^{-1} \left(\frac{\mathbf{e} \cdot \frac{\mathbf{r}}{r}}{e} \right).$$

In the perturbed two-body problem the motion is not keplerian and \mathbf{h} , \mathbf{e} , ϑ_0 , defined by Eqs. (2) - (4), vary, in general, along the trajectory. These quantities are called *osculating* because at each time t they characterize the osculating keplerian orbit tangent in P to the particle trajectory, as shown in Fig. (1). The *variation of parameters* methods provide a system of differential equations for the osculating elements, which become the new state variables.

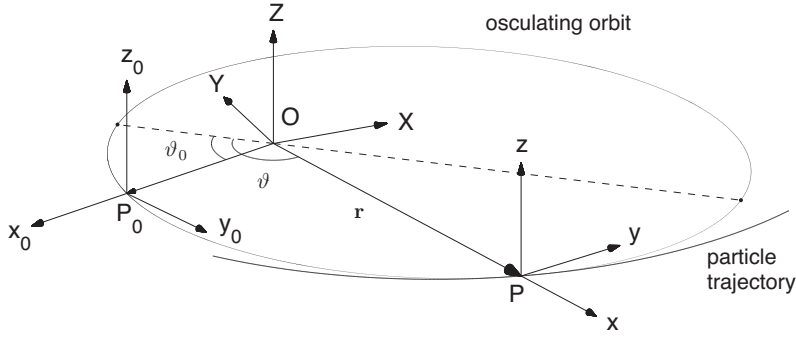


Figure 1. Osculating keplerian orbit tangent in P to the particle trajectory (the dashed line is the apside line), and reference frames \mathcal{I} , \mathcal{R}_0 and \mathcal{R} .

From time to a new independent variable

Peláez et al. [1] introduce a change of the independent variable from time t to fictitious time σ , similar to the Sundman transformation (see ref. [10]), which is the first step in the regularization process of the two-body problem

$$\frac{dt}{d\sigma} = \frac{r^2}{h}. \quad (5)$$

If the integrand in Eq. (4) is expressed, through Eq. (5), as the time derivative of σ , and then we solve for ϑ , we have

$$\vartheta = \vartheta_0 + \sigma - \sigma_0 \quad (6)$$

where σ_0 is an arbitrary constant. Eq. (6) is important because it allows to determine ϑ without solving Kepler's equation. The special perturbation method [1] exploits this relation to derive the equations of motion.

A new set of integrals of the two-body problem

We define the new set of integrals, or osculating elements, chosen by Peláez et al. [1], in terms of h , e , and ϑ_0 introduced in Eqs. (2) - (4). The constants r_0 and ω_0 are used in [1] to obtain non-dimensional length and time

$$r_0 = \|\mathbf{r}_0\|$$

$$\omega_0 = \sqrt{\frac{\mu}{r_0^3}}.$$

The first three quantities determine the shape and the initial true anomaly of the real or osculating keplerian orbit. They take the form

$$q_1 = f(h, e, \vartheta_0) = \frac{e}{\tilde{h}} \cos(\sigma_0 - \vartheta_0) \quad (7)$$

$$q_2 = f(h, e, \vartheta_0) = \frac{e}{\tilde{h}} \sin(\sigma_0 - \vartheta_0) \quad (8)$$

$$q_3 = f(h) = \frac{1}{\tilde{h}} \quad (9)$$

where \tilde{h} is the non-dimensional specific angular momentum

$$\tilde{h} = \frac{h}{r_0^2 \omega_0}. \quad (10)$$

The next quantities arrange the inertial orientation of the orbit. We introduce the orbital frame $\mathcal{R}_0 = \{P_0; \mathbf{i}_{x_0}, \mathbf{i}_{y_0}, \mathbf{i}_{z_0}\}$ shown in Fig. (1): the origin is placed in P_0 , the x_0 -axis is in the same direction of OP_0 , the z_0 -axis is in the same direction of the orbit angular momentum vector and the y_0 -axis completes the right-handed frame. Euler's theorem on the motion of a rigid body ensures that, if \mathcal{R}_0 is translated from P_0 to O , \mathcal{R}_0 can be superimposed to the inertial frame \mathcal{I} through a rotation of ϕ_0 around some axis \mathbf{a}_0 . We take as integrals the four components $\varepsilon_{10}, \varepsilon_{20}, \varepsilon_{30}, \eta_0$ of the unit quaternion which represents this transformation between \mathcal{R}_0 and \mathcal{I} as

$$\varepsilon_0 = \mathbf{a}_0 \sin \frac{\phi_0}{2} = \varepsilon_{10} \mathbf{i}_{x_0} + \varepsilon_{20} \mathbf{i}_{y_0} + \varepsilon_{30} \mathbf{i}_{z_0} \quad \eta_0 = \cos \frac{\phi_0}{2},$$

and the corresponding rotation matrix from \mathcal{R}_0 to \mathcal{I} is

$$\mathbf{Q}_0 = \begin{bmatrix} 1 - 2\varepsilon_{20}^2 - 2\varepsilon_{30}^2 & 2\varepsilon_{10}\varepsilon_{20} - 2\eta_0\varepsilon_{30} & 2\varepsilon_{10}\varepsilon_{30} + 2\eta_0\varepsilon_{20} \\ 2\varepsilon_{10}\varepsilon_{20} + 2\eta_0\varepsilon_{30} & 1 - 2\varepsilon_{10}^2 - 2\varepsilon_{30}^2 & 2\varepsilon_{20}\varepsilon_{30} - 2\eta_0\varepsilon_{10} \\ 2\varepsilon_{10}\varepsilon_{30} - 2\eta_0\varepsilon_{20} & 2\varepsilon_{20}\varepsilon_{30} + 2\eta_0\varepsilon_{10} & 1 - 2\varepsilon_{10}^2 - 2\varepsilon_{20}^2 \end{bmatrix}. \quad (11)$$

After introducing the vector

$$\mathbf{p} = p \mathbf{u}_p = \mathbf{h} \times \mathbf{e}$$

where p and \mathbf{u}_p are the magnitude and the direction of \mathbf{p} , the quaternion components take the form

$$\varepsilon_{10} = f_4(\mathbf{u}_h, \mathbf{u}_e, \vartheta_0) = \frac{1}{4\eta_0} \{u_{pZ} \cos \vartheta_0 - u_{eZ} \sin \vartheta_0 - u_{hY}\} \quad (12)$$

$$\varepsilon_{20} = f_5(\mathbf{u}_h, \mathbf{u}_e, \vartheta_0) = \frac{1}{4\eta_0} \{-u_{eZ} \cos \vartheta_0 - u_{pZ} \sin \vartheta_0 + u_{hX}\} \quad (13)$$

$$\varepsilon_{30} = f_6(\mathbf{u}_h, \mathbf{u}_e, \vartheta_0) = \frac{1}{4\eta_0} \{(u_{eY} - u_{pX}) \cos \vartheta_0 + (u_{eX} + u_{pY}) \sin \vartheta_0\} \quad (14)$$

$$\eta_0 = f_7(\mathbf{u}_h, \mathbf{u}_e, \vartheta_0) = \frac{1}{2} \sqrt{(u_{eX} + u_{pY}) \cos \vartheta_0 - (u_{eY} - u_{pX}) \sin \vartheta_0 + 1 + u_{hZ}}. \quad (15)$$

Eqs. (7) - (9) and (12) - (15) are useful to initialize the variables for the integration, but they are not implemented inside the integration method. Note that Eqs. (12) - (15) contain a singularity when $\eta_0 = 0$, alternative expressions for this case are reported in Appendix A.

To summarize, the new set of integrals is

$$\boldsymbol{\alpha} = (q_1 \quad q_2 \quad q_3 \quad \varepsilon_{10} \quad \varepsilon_{20} \quad \varepsilon_{30} \quad \eta_0)^T,$$

only six of them are independent, because the unit quaternion satisfies the condition

$$\varepsilon_{10}^2 + \varepsilon_{20}^2 + \varepsilon_{30}^2 + \eta_0^2 = 1. \quad (16)$$

Relations for the orbital elements in terms of $\boldsymbol{\alpha}$ are derived in Appendix B.

From the new set of integrals to the particle position and velocity vectors

Let us consider the particle position P at time t . We introduce the orbital frame $\mathcal{R} = \{P; \mathbf{i}_x, \mathbf{i}_y, \mathbf{i}_z\}$ shown in Fig. (1): the origin is placed in P , the x -axis is in the same direction of \mathbf{r} , the z -axis is in the same direction of the orbit angular momentum vector and the y -axis completes the right-handed frame.

The particle position and velocity vectors projected on \mathcal{R} take the form

$$\mathbf{r} = (r \quad 0 \quad 0)^T$$

$$\dot{\mathbf{r}} = (v_r \quad v_t \quad 0)^T$$

where the orbital radius r , the radial velocity v_r and the transverse velocity v_θ are expressed in function of h , e and ϑ through the equations (see ref. [11], pp. 117 and 126)

$$r = \frac{h^2}{\mu(1 + e \cos \vartheta)} \quad (17)$$

$$v_r = \frac{\mu}{h} e \sin \vartheta \quad (18)$$

$$v_\theta = \frac{\mu}{h} (1 + e \cos \vartheta) . \quad (19)$$

Eqs. (51) and (52) in Appendix B are exploited to write Eqs. (17) - (19) as follows

$$r = \frac{r_0}{q_3 \left(\sqrt{q_1^2 + q_2^2} \cos \vartheta + q_3 \right)} \quad (20)$$

$$v_r = r_0 \omega_0 \sqrt{q_1^2 + q_2^2} \sin \vartheta \quad (21)$$

$$v_\theta = r_0 \omega_0 \left(\sqrt{q_1^2 + q_2^2} \cos \vartheta + q_3 \right) . \quad (22)$$

The true anomaly can be determined without solving Kepler's equation: we substitute ϑ_0 in Eq. (6) with the expression given in Eq. (55) in Appendix B to yield

$$\vartheta = \sigma - \tan^{-1} \frac{q_2}{q_1} . \quad (23)$$

Eq. (23) is used in Eqs. (20) - (22) and after some trigonometric operations we have

$$r = \frac{r_0}{q_3 s} \quad (24)$$

$$v_r = r_0 \omega_0 (q_1 \sin \sigma - q_2 \cos \sigma) \quad (25)$$

$$v_\theta = r_0 \omega_0 s \quad (26)$$

where s is the non-dimensional transverse velocity

$$s = q_1 \cos \sigma + q_2 \sin \sigma + q_3 .$$

Finally, \mathbf{r} and $\dot{\mathbf{r}}$ are projected on the inertial frame \mathcal{I} . The rotation matrix from \mathcal{R} to \mathcal{I} is computed as

$$\mathbf{Q} = \mathbf{Q}_0 \mathbf{M} \quad (27)$$

where \mathbf{Q}_0 is defined in Eq. (11) and \mathbf{M} is the rotation matrix from \mathcal{R} to \mathcal{R}_0

$$\mathbf{M} = \begin{bmatrix} \cos(\sigma - \sigma_0) & -\sin(\sigma - \sigma_0) & 0 \\ \sin(\sigma - \sigma_0) & \cos(\sigma - \sigma_0) & 0 \\ 0 & 0 & 1 \end{bmatrix}$$

Note that \mathcal{R} and \mathcal{R}_0 are rotated one respect to the other of $\vartheta - \vartheta_0$ in the orbital plane, and this angle is equal to $\sigma - \sigma_0$, as can be checked by rearranging the terms in Eq. (6).

Equations of motion

The Poisson's variational method (see ref. [11], pp. 495-497) is used to determine the derivatives of the new set of osculating elements contained in α respect to the independent variable σ , according to the equation

$$\frac{d\alpha}{d\sigma} = \frac{dt}{d\sigma} \frac{\partial \alpha}{\partial \mathbf{f}} \mathbf{a}_p \quad (28)$$

where

$$\tilde{\mathbf{a}}_p = \frac{\mathbf{F}_p}{m r_0 \omega_0^2}$$

is the non-dimensional perturbative acceleration vector. The variational equations of motion are derived in Appendix C and take the form

$$\frac{dq_1}{d\sigma} = \frac{1}{q_3 s^2} \left\{ \tilde{\mathbf{a}}_p \cdot \mathbf{i}_x \sin \sigma + \left(1 + \frac{q_3}{s} \right) \tilde{\mathbf{a}}_p \cdot \mathbf{i}_y \cos \sigma \right\} \quad (29)$$

$$\frac{dq_2}{d\sigma} = \frac{1}{q_3 s^2} \left\{ -\tilde{\mathbf{a}}_p \cdot \mathbf{i}_x \cos \sigma + \left(1 + \frac{q_3}{s} \right) \tilde{\mathbf{a}}_p \cdot \mathbf{i}_y \sin \sigma \right\} \quad (30)$$

$$\frac{dq_3}{d\sigma} = -\frac{1}{s^3} \tilde{\mathbf{a}}_p \cdot \mathbf{i}_y \quad (31)$$

$$\frac{d\varepsilon_{10}}{d\sigma} = +\frac{\tilde{\mathbf{a}}_p \cdot \mathbf{i}_z}{2q_3 s^3} \{ \eta_0 \cos \Delta\sigma - \varepsilon_{30} \sin \Delta\sigma \} \quad (32)$$

$$\frac{d\varepsilon_{20}}{d\sigma} = +\frac{\tilde{\mathbf{a}}_p \cdot \mathbf{i}_z}{2q_3 s^3} \{ \varepsilon_{30} \cos \Delta\sigma + \eta_0 \sin \Delta\sigma \} \quad (33)$$

$$\frac{d\varepsilon_{30}}{d\sigma} = -\frac{\tilde{\mathbf{a}}_p \cdot \mathbf{i}_z}{2q_3 s^3} \{ \varepsilon_{20} \cos \Delta\sigma - \varepsilon_{10} \sin \Delta\sigma \} \quad (34)$$

$$\frac{d\eta_0}{d\sigma} = -\frac{\tilde{\mathbf{a}}_p \cdot \mathbf{i}_z}{2q_3 s^3} \{ \varepsilon_{10} \cos \Delta\sigma + \varepsilon_{20} \sin \Delta\sigma \} \quad (35)$$

where $\Delta\sigma = \sigma - \sigma_0$.

Because it may be required in the calculation of $\tilde{\mathbf{a}}_p$, time is also an integration variable. From Eq. (5) and employing Eq. (24) and Eq. (52) in Appendix B, we write the differential equation for time in terms of σ and q_1, q_2, q_3

$$\frac{dt}{d\sigma} = \frac{1}{\omega_0 q_3 s^2}. \quad (36)$$

Eqs. (29) - (36) constitute the system of differential equations that governs the perturbed two-body motion of one point mass. They are integrated with the proper initial conditions in the selected interval of the independent variable. If the components of $\tilde{\mathbf{a}}_p$ are known in the inertial frame, the application of the inverse of the rotation matrix \mathbf{Q} in Eq. (27) is necessary.

The special perturbation method [1] is singular when $s = 0$ or $q_3 s = 0$. The first case appears when the motion is rectilinear, the second case when the orbital radius grows up to infinite, but the disturbing accelerations are different from zero. Both situations are unusual in orbital dynamics.

FORMATION FLIGHT

Let us consider n spacecraft in formation flight around a primary, and let $\mathcal{I} = \{O; \mathbf{i}_X, \mathbf{i}_Y, \mathbf{i}_Z\}$ be an inertial frame with the origin placed at the primary center of mass. At time t_0 the dynamic state of each spacecraft is given by the inertial position and velocity vectors \mathbf{r}_0 and $\dot{\mathbf{r}}_0$. The problem of determining the time evolution of the formation is usually stated in these terms: *propagate the relative dynamic states of the spacecraft respect to a reference orbit, and propagate this orbit*. The reference spacecraft (real or virtual) should be chosen in such a way that represents the formation position in space, and the spacecraft relative positions can be easily understood. This formulation of the problem is suitable for planning station keeping and formation keeping control strategies.

We propose two approaches to determine the relative motion of the spacecraft respect to the formation center of mass. In the first we apply the special perturbation method [1] to each spacecraft, in the second only to the center of mass.

First model

The special perturbation method [1] is applied to each spacecraft to obtain a synchronous propagation of its relative dynamic states respect to the formation center of mass.

If Eqs. (29) - (36) are integrated for the n masses in the same independent variable σ , we calculate, in general, the position and velocity vectors of the spacecraft at different times for each integration step. In order to overcome this difficulty, we first assume a unique time imposed by a generic mass of the formation, for instance mass 1

$$t_1 = t_i \quad i = 2, \dots, n.$$

As a consequence σ will take, in general, a different value for each spacecraft at the same time t_1 , as can be inferred from the equation

$$\frac{d\sigma_i}{dt_1} = \omega_0 q_{3,i} s_i^2 \quad i = 1, \dots, n \quad (37)$$

derived from Eq. (36). Then, after introducing the n variables σ_i , we assume σ_1 as the independent variable and the other quantities σ_i as new integration variables. Thus, we write one differential equation for time

$$\frac{dt_1}{d\sigma_1} = \frac{1}{\omega_0 q_{3,1} s_1^2}, \quad (38)$$

the $n - 1$ differential equations

$$\frac{d\sigma_i}{d\sigma_1} = \frac{d\sigma_i}{dt_1} \frac{dt_1}{d\sigma_1} = \frac{q_{3,i} s_i^2}{q_{3,1} s_1^2} \quad i = 2, \dots, n \quad (39)$$

where Eqs. (37) and (38) have been exploited, and the $7n$ variational equations

$$\frac{d\alpha_i}{d\sigma_1} = \frac{q_{3,i} s_i^2}{q_{3,1} s_1^2} \frac{d\alpha_i}{d\sigma_i} \quad i = 1, \dots, n \quad (40)$$

where the term $d\alpha_i/d\sigma_i$ on the right hand represents the set of Eqs. (29) - (35) for the i -th mass. By integrating the $8n$ Eqs. (38) - (40) we propagate the motion of the spacecraft at the same times. The dynamic state of the center of mass is computed by the formula

$$\mathbf{s}_G = \frac{1}{M} \sum_{i=1}^n m_i \mathbf{s}_i$$

where M is the formation total mass given by $\sum_{i=1}^n m_i$, and \mathbf{s}_i contains the dynamic state of the i -th spacecraft. Finally, the relative dynamic states of the spacecraft respect to the center of mass are determined by the difference

$$\delta \mathbf{s}_i = \mathbf{s}_i - \mathbf{s}_G \quad i = 1, \dots, n.$$

Second model

The absolute motion of each spacecraft is the composition of the reference mass translational motion, and the relative motion respect to this mass. Let us choose the formation center of mass G as the reference point of mass M , equal to the total mass of the formation. The position (\mathbf{r}) and velocity (\mathbf{v}) vectors of each spacecraft take the form

$$\begin{aligned} \mathbf{r} &= \mathbf{r}_G + \delta \mathbf{r} \\ \mathbf{v} &= \mathbf{v}_G + \delta \mathbf{v} \end{aligned} \quad (41)$$

where $\delta \mathbf{r}$ and $\delta \mathbf{v}$ are the relative position and velocity vectors respect to the center of mass. The time derivatives of \mathbf{r} and \mathbf{v} are

$$\begin{aligned}\frac{d\mathbf{r}}{dt} &= \mathbf{v} \\ \frac{d\mathbf{v}}{dt} &= -\frac{\mu}{r^3}\mathbf{r} + \mathbf{g}_p(\mathbf{r}) + \mathbf{a}_p(\mathbf{r}, \mathbf{v}, t)\end{aligned}\quad (42)$$

where the vector \mathbf{g}_p includes the perturbative gravitational effects under consideration, and \mathbf{a}_p is the resultant vector of the perturbative non-gravitational accelerations, which, in general, can be external or internal to the formation

$$\mathbf{a}_p(\mathbf{r}, \mathbf{v}, t) = \mathbf{a}_p^{\text{ext}}(\mathbf{r}, \mathbf{v}, t) + \mathbf{a}_p^{\text{int}}(\mathbf{r}, \mathbf{v}, t) .$$

The center of mass dynamic state varies according to the equations

$$\begin{aligned}\frac{d\mathbf{r}_G}{dt} &= \mathbf{v}_G \\ \frac{d\mathbf{v}_G}{dt} &= \frac{1}{M} \sum_{i=1}^n m_i \left\{ -\frac{\mu}{r_i^3}\mathbf{r}_i + \mathbf{g}_{p,i}(\mathbf{r}_i) + \mathbf{a}_{p,i}^{\text{ext}}(\mathbf{r}_i, \mathbf{v}_i, t) \right\},\end{aligned}\quad (43)$$

and in order to propagate its motion through the special perturbation method [1], we need to find a two-body problem formulation of Eq. (43). Let us expand the gravitational terms in Eq. (42) about the reference path with Taylor's theorem. Stopping at the first order, we get

$$-\frac{\mu}{r^3}\mathbf{r} + \mathbf{g}_p(\mathbf{r}) = -\frac{\mu}{r_G^3}\mathbf{r}_G + \mathbf{g}_p(\mathbf{r}_G) + [\mathbf{G}(\mathbf{r}_G) + \mathbf{G}_p(\mathbf{r}_G)]\boldsymbol{\delta} + \mathcal{O}(\boldsymbol{\delta}^2)\quad (44)$$

where $\mathbf{G}(\mathbf{r}_G)$ and $\mathbf{G}_p(\mathbf{r}_G)$ are the gravity gradient matrix and the gradient matrix of the perturbative gravitational accelerations calculated at the center of mass position vector

$$\mathbf{G}(\mathbf{r}_G) + \mathbf{G}_p(\mathbf{r}_G) = \left. \frac{d}{d\mathbf{r}} \left\{ -\frac{\mu}{r^3}\mathbf{r} + \mathbf{g}_p(\mathbf{r}) \right\} \right|_{\mathbf{r}=\mathbf{r}_G} .$$

By substituting Eq. (44) into Eq. (43), we obtain

$$\frac{d\mathbf{v}_G}{dt} = \frac{1}{M} \sum_{i=1}^n m_i \left\{ -\frac{\mu}{r_G^3}\mathbf{r}_G + \mathbf{g}_p(\mathbf{r}_G) + [\mathbf{G}(\mathbf{r}_G) + \mathbf{G}_p(\mathbf{r}_G)]\boldsymbol{\delta}_i + \mathcal{O}(\boldsymbol{\delta}_i^2) + \mathbf{a}_{p,i}^{\text{ext}}(\mathbf{r}_i, \mathbf{v}_i, t) \right\}$$

and after applying the definition of the center of mass position vector, the previous equation becomes

$$\frac{d\mathbf{v}_G}{dt} = -\frac{\mu}{r_G^3}\mathbf{r}_G + \mathbf{g}_p(\mathbf{r}_G) + \frac{1}{M} \sum_{i=1}^n m_i [\mathcal{O}(\boldsymbol{\delta}_i^2) + \mathbf{a}_{p,i}^{\text{ext}}(\mathbf{r}_i, \mathbf{v}_i, t)] .\quad (45)$$

Comparing Eq. (45) with Eq. (42), we see that they appear in the same form: the center of mass behaves like a particle of mass M moving around the primary under the influence of the perturbative acceleration vector

$$\mathbf{a}_{G,p} = \mathbf{g}_p(\mathbf{r}_G) + \frac{1}{M} \sum_{i=1}^n m_i [\mathcal{O}(\boldsymbol{\delta}_i^2) + \mathbf{a}_{p,i}^{\text{ext}}(\mathbf{r}_i, \mathbf{v}_i, t)] .$$

Therefore, Eqs. (29) - (36) can be integrated with the non-dimensional perturbative acceleration given by

$$\tilde{\mathbf{a}}_{G,p} = \frac{\mathbf{a}_{G,p}}{r_{G,0} \omega_{G,0}^2} .$$

Let us derive the equations which govern the relative dynamics of the spacecraft respect to the center of mass. We substitute Eq. (44) into Eq. (42) to get

$$\frac{d\mathbf{v}}{dt} = -\frac{\mu}{r_G^3}\mathbf{r}_G + \mathbf{g}_p(\mathbf{r}_G) + [\mathbf{G}(\mathbf{r}_G) + \mathbf{G}_p(\mathbf{r}_G)]\boldsymbol{\delta} + \mathcal{O}(\boldsymbol{\delta}^2) + \mathbf{a}_p(\mathbf{r}, \mathbf{v}, t) ,\quad (46)$$

Table 1. Center of mass initial orbit: perigee radius (r_p), eccentricity (e), inclination (i), argument of perigee (ω), right ascension (Ω), initial true anomaly (ϑ_0 , for the circular orbit it is the angle between the node vector and the position vector).

Orbit	r_p [km]	e	i [deg]	ω [deg]	Ω [deg]	ϑ_0 [deg]
1)	42241	0	30	–	0	0
2)	21121	0.5	30	0	0	0
3)	7040	0	30	–	0	0
4)	7040	0.5	30	0	0	0

when Eq. (41) is differentiated respect to time and Eqs. (45) and (46) are employed, the relative acceleration vector of a generic spacecraft respect to the center of mass takes the form

$$\frac{d\delta\mathbf{v}}{dt} = [\mathbf{G}(\mathbf{r}_G) + \mathbf{G}_p(\mathbf{r}_G)] \delta + \mathcal{O}(\delta^2) + \mathbf{a}_p(\mathbf{r}, \mathbf{v}, t) - \frac{1}{M} \sum_{i=1}^n m_i [\mathcal{O}(\delta_i^2) + \mathbf{a}_{p,i}^{\text{ext}}(\mathbf{r}_i, \mathbf{v}_i, t)] . \quad (47)$$

Eq. (47) and equation

$$\frac{d\delta\mathbf{r}}{dt} = \delta\mathbf{v} \quad (48)$$

describe the time evolution of the relative dynamic state of each spacecraft. We prefer to evaluate $\delta\mathbf{r}$ and $\delta\mathbf{v}$ in the inertial frame $\mathcal{I} = \{G; \mathbf{i}_X, \mathbf{i}_Y, \mathbf{i}_Z\}$, instead of the orbital frame $\mathcal{R} = \{G; \mathbf{i}_x, \mathbf{i}_y, \mathbf{i}_z\}$, to avoid the non-trivial determination of the time derivative of $\tilde{\mathbf{a}}_{G,p}$, which appears in the x component of the angular velocity vector of \mathcal{R}

$$w_x = \frac{\omega_{G,0}}{s} (\tilde{\mathbf{a}}_{G,p} \cdot \mathbf{i}_z) .$$

Because the independent variable is σ and not t , Eqs. (47) and (48) are multiplied by Eq. (36).

Note that, if an external perturbative acceleration vector has the same magnitude and direction for all the spacecraft, it disappears from Eq. (47) because it does not produce a differential effect on the formation relative dynamics.

RESULTS

Let us call P1 and P2 the first and the second model. They are compared in terms of computational speed taking an example of a formation similar to that used in LISA (Laser Interferometer Space Antenna) mission: three spacecraft of the same mass m which fly around the Earth in a triangular formation with arms of equal length l .

The motions of the spacecraft are propagated by P1 and P2, first without applying perturbations and then adding the perturbative forces due to the Earth oblateness and the Lunar third-body effect. In the model P2 the perturbations take into account the first order in the Taylor expansions of these forces.

The spacecraft initial position and velocity vectors in the model P1 are calculated from the initial dynamic state of the formation center of mass, which is specified by the keplerian orbits reported in Table (1): two geosynchronous orbits (GEO) and two low Earth orbits (LEO). In the next two sections we explain how the initial relative position and velocity vectors of the spacecraft respect to the center of mass are obtained.

Circular reference orbit

Let us consider a circular orbit for the center of mass. When the motion of the spacecraft is unperturbed, the model P2 numerically integrates the Clohessy-Wiltshire (CW) equations written respect to the center of mass of the triangle in an inertial frame attached to G . In the CW hypothesis the triangle can rotate like a rigid body around a fix spinning axis normal to the plane where it lies, if the following conditions are applied to the formation:

Table 2. Initial relative positions and velocities of the spacecraft A , B and C in the orbital frame \mathcal{R} for a circular reference orbit.

S/C	A	B	C
$\delta r_{x,0}$ [km]	$l\sqrt{3}/6$	$-l\sqrt{3}/12$	$-l\sqrt{3}/12$
$\delta r_{y,0}$ [km]	0	$l/2$	$-l/2$
$\delta r_{z,0}$ [km]	$l/2$	$-l/4$	$-l/4$
$\delta v_{x,0}$ [km/s]	0	$lw_E/4$	$-lw_E/4$
$\delta v_{y,0}$ [km/s]	$-lw_E\sqrt{3}/3$	$lw_E\sqrt{3}/6$	$lw_E\sqrt{3}/6$
$\delta v_{z,0}$ [km/s]	0	$lw_E\sqrt{3}/4$	$-lw_E\sqrt{3}/4$

1. The relative motion is bounded, which is realized by the constraint

$$\delta v_{y,0}^{(i)} = -2w_E\delta r_{x,0}^{(i)} \quad i = 1, 2, 3$$

where w_E is the Earth angular velocity around its rotation axis.

2. The motion at time t_0 , in the orbital frame $\mathcal{R} = \{G; \mathbf{i}_x, \mathbf{i}_y, \mathbf{i}_z\}$, is a rigid rotation around an axis normal to the plane where the formation lies, and the angular velocity of this rotation coincides with w_E .

The combination of these conditions determines the values $\pm 60^\circ$ as the only two possible inclinations of the triangle plane respect to the reference orbital plane. We choose here the hyperbolic configuration given by the angle $+60^\circ$. The initial relative position and velocity vectors of the spacecraft in the orbital frame \mathcal{R} are contained in Table (2).

Elliptical reference orbit

Let us consider an elliptical orbit for the center of mass. When the motion of the spacecraft is unperturbed, the model P2 numerically integrates the Tschauner-Hempel [12] equations written respect to the center of mass of the triangle in an inertial frame attached to G . In order to get bounded motion near the reference orbit, we apply to each mass the constraint (see ref. [13])

$$\delta v_{y,0}^{(i)} = -\frac{n(2+e)}{\sqrt{(1+e)(1-e)^3}}\delta r_{x,0}^{(i)} \quad i = 1, 2, 3 \quad (49)$$

where n and e are the mean motion and the eccentricity of the reference orbit. Eq. (49) works only when the initial position of the center of mass is at perigee. Eccentricity does not allow a rigid motion of the triangle around a spinning axis like in the circular case. Without performing any optimization on the initial conditions, we only impose that, in the orbital frame \mathcal{R} , the motion at time t_0 is a rigid rotation around the axis normal to the triangle plane, and the angular velocity of this rotation coincides with the angular velocity at perigee w_p . The initial relative position and velocity vectors of the spacecraft in the orbital frame \mathcal{R} are the same contained in Table (2), where ω_E is replaced by w_p .

After initializing the integration variables, we start the integration in the following ranges of the independent variable σ

$$\Delta\sigma_{\text{GEO}} = \sigma_f - \sigma_0 = 30 \times 2\pi \text{ rad}$$

$$\Delta\sigma_{\text{LEO}} = \sigma_f - \sigma_0 = 15 \times 2\pi \text{ rad}$$

where σ_f is the final value taken by σ and σ_0 is chosen to be the initial true anomaly. Remember that σ in the model P1 refers to one of the masses of the formation, while in the model P2 to the center of mass. A Runge-Kutta fourth order numerical integrator is used.

Table 3. Comparison of the times of integration of P1 and P2 for the orbit 1 of Tab. (1).

	Unperturbed motion		Perturbed motion	
	t_{P1} [s]	t_{P2} [s]	t_{P1} [s]	t_{P2} [s]
$l_{1,GEO}$	1.6055	98.4738	11.1963	104.4350
$l_{2,GEO}$	1.7520	99.9208	11.2699	105.6100
$l_{3,GEO}$	1.8421	101.3234	11.3001	104.9073

Table 4. Comparison of the times of integration of P1 and P2 for the orbit 2 of Tab. (1).

	Unperturbed motion		Perturbed motion	
	t_{P1} [s]	t_{P2} [s]	t_{P1} [s]	t_{P2} [s]
$l_{1,GEO}$	8.6281	99.9242	13.8969	104.2881
$l_{2,GEO}$	8.5977	100.3348	13.8702	104.2245
$l_{3,GEO}$	8.5957	100.6011	13.7653	120.4167

Table 5. Comparison of the times of integration of P1 and P2 for the orbit 3 of Tab. (1).

	Unperturbed motion		Perturbed motion	
	t_{P1} [s]	t_{P2} [s]	t_{P1} [s]	t_{P2} [s]
$l_{1,LEO}$	1.1468	43.0834	11.5984	45.2400
$l_{2,LEO}$	1.4779	44.3962	11.5750	45.8455
$l_{3,LEO}$	1.2829	45.0691	11.5718	46.4105

Table 6. Comparison of the times of integration of P1 and P2 for the orbit 4 of Tab. (1).

	Unperturbed motion		Perturbed motion	
	t_{P1} [s]	t_{P2} [s]	t_{P1} [s]	t_{P2} [s]
$l_{1,LEO}$	5.1352	46.6060	9.2219	47.9290
$l_{2,LEO}$	5.0999	46.9792	9.2405	48.4895
$l_{3,LEO}$	5.0949	47.1498	9.2294	48.8311

Table 7. Comparison of the times of integration of P1 and P2 for the orbit 1 of Tab. (1) with an increasing number of orbits ($l = 5$ km).

N. orbits	Unperturbed motion		Perturbed motion	
	t_{P1} [s]	t_{P2} [s]	t_{P1} [s]	t_{P2} [s]
150	12.94	466.42	60.05	519.47
300	15.44	980.18	113.71	1066.71
450	18.59	1591.20	171.46	1776.37
600	22.28	2250.02	231.17	2349.83

In Tables (3) - (6) we compare the times of integration of P1 and P2 for the four orbits of Table (1). For each orbit three different initial arm lengths are considered

$$\begin{aligned}
 l_{1,GEO} &= 9 \text{ km} & l_{1,LEO} &= 1.5 \text{ km} \\
 l_{2,GEO} &= 18 \text{ km} & l_{2,LEO} &= 3 \text{ km} \\
 l_{3,GEO} &= 27 \text{ km} & l_{3,LEO} &= 4.5 \text{ km} .
 \end{aligned}$$

We note that:

- model P1 is always faster than model P2, and the difference in the integration times is particularly evident when the motion is unperturbed;
- model P2 is not very sensitive to eccentricity both in the unperturbed and in the perturbed motion;
- perturbations have a bigger impact on the times of integration of model P1 than model P2.

In Table (7) we show the times of integration for the geosynchronous circular orbit obtained with models P1 and P2 for an increasing number of orbits and an arm length of 5 km. Note that the integration times increase proportionally to the number of orbits, except when model P1 is used in the unperturbed problem. In this case the difference between the two models in terms of computational times grows with the number of orbits.

Finally, we checked that the times of integration of model P1 are nearly equal to three times the time of integration of one single mass of the formation. This means that the additional Eqs. (39) introduced in the model P1 in order to synchronize the orbital propagations do not affect the total time of integration.

The model P1 is not only very fast, but also accurate in the determination of the absolute dynamic states of the spacecraft (see ref. [1]). However, it presents two disadvantages respect to the slower and less accurate model P2:

1. It suffers from the round-off error: if the formation dimension is very small compared to the center of mass distance from the primary, then the round-off error can affect the calculation of the relative position and velocity vectors. On the contrary P2 becomes more accurate.
2. It does not give information on the effect of single perturbation terms on the formation relative dynamics.

CONCLUSIONS

The fast and accurate special perturbation method developed in 2006 by Peláez et al. [1] is used to propagate the relative motion of a formation flight. We propose two different models: P1 and P2. In model P1, the special perturbation method is applied to each spacecraft. In model P2 the gravitational terms appearing

in the two-body equations of motion are expanded respect to a reference orbit given by the center of mass. This operation allows to write the center of mass equation of motion like a two body equation. Thus, we apply to the center of mass the special perturbation method [1] and we describe the relative dynamics of the spacecraft respect to a reference frame moving with the center of mass but with an inertial attitude. We compare the times of integration of the models when applied to a triangular formation with bounded initial motion imposed to the spacecraft. Model P1 proves to be faster than model P2, and the difference in the time of integration is more evident when no perturbations are applied and the number of orbits is very high. This model (P1), for its computational velocity could be used in an onboard computer for relative motion prediction.

APPENDIX A: ALTERNATIVE EXPRESSIONS OF ε_0 WHEN η_0 IS EQUAL TO ZERO

If $\eta_0 = 0$ Eqs. (12) - (14) become singular. In this case ε_0 coincides with the rotation axis \mathbf{a}_0 , and its components can be calculated by the relations

$$\varepsilon_{10} = \frac{u_{hX}}{2\varepsilon_{30}} \quad \varepsilon_{20} = \frac{u_{hY}}{2\varepsilon_{30}} \quad \varepsilon_{30} = \sqrt{\frac{u_{hZ} + 1}{2}} .$$

If besides $u_{hZ} = -1$, then $\varepsilon_{30} = 0$ and $\varepsilon_{10}, \varepsilon_{20}$ are singular. In order to overcome the singularity, we use the relations

$$\varepsilon_{10} = \sqrt{\frac{1 + u_{eX} \cos \vartheta_0 + u_{pX} \sin \vartheta_0}{2}} \quad \varepsilon_{20} = \frac{u_{pX} \cos \vartheta_0 - u_{eX} \sin \vartheta_0}{2\varepsilon_{10}} .$$

Finally, note that if $\varepsilon_{10} = 0$ the expression for ε_{20} is singular. This situation occurs when \mathbf{a}_0 has the same direction of either $+\mathbf{i}_Y$ or $-\mathbf{i}_Y$. In these two particular cases the quaternion components take the values

$$\varepsilon_{10} = 0 \quad \varepsilon_{20} = \pm 1 \quad \varepsilon_{30} = 0 \quad \eta_0 = 0 .$$

APPENDIX B: ORBITAL ELEMENTS IN TERMS OF THE NEW SET OF INTEGRALS

Semi-major axis We sum q_1 and q_2 both squared and exploit Eqs. (7) and (8) to obtain

$$q_1^2 + q_2^2 = \left(\frac{e}{\tilde{h}}\right)^2 . \quad (50)$$

From the previous result we subtract q_3 squared and using Eq. (9) we have

$$q_1^2 + q_2^2 - q_3^2 = \frac{e^2 - 1}{\tilde{h}^2} ,$$

by substituting \tilde{h} with $\sqrt{a(1-e^2)}/r_0$ and solving for the semi-major axis, we find

$$a = \frac{r_0}{q_3^2 - q_1^2 - q_2^2} .$$

Eccentricity Plugging Eq. (9) into Eq. (50) and solving for e , yields

$$e = \frac{\sqrt{q_1^2 + q_2^2}}{q_3} . \quad (51)$$

Specific angular momentum Plugging Eq. (10) into Eq. (9) and solving for h , yields

$$h = \frac{r_0^2 \omega_0}{q_3} . \quad (52)$$

Inclination The rotation matrix associated to the unit quaternion ε_0, η_0 in Eq. (11) can be expressed in function of the inclination i , the right ascension Ω , the initial true anomaly ϑ_0 and the argument of perigee ω as follows

$$\mathbf{Q}_0 = \begin{bmatrix} \cos \Omega \cos \bar{\omega} - \sin \Omega \sin \bar{\omega} \cos i & -\cos \Omega \sin \bar{\omega} - \sin \Omega \cos \bar{\omega} \cos i & \sin \Omega \sin i \\ \sin \Omega \cos \bar{\omega} + \cos \Omega \sin \bar{\omega} \cos i & -\sin \Omega \sin \bar{\omega} + \cos \Omega \cos \bar{\omega} \cos i & -\cos \Omega \sin i \\ \sin \bar{\omega} \sin i & \cos \bar{\omega} \sin i & \cos i \end{bmatrix} \quad (53)$$

where $\bar{\omega} = \omega + \vartheta_0$. The element $Q_{0,33}$ in Eqs. (11) and (53) is used to derive the relation

$$i = \cos^{-1} [1 - 2(\varepsilon_{10}^2 + \varepsilon_{20}^2)].$$

Right ascension of the ascending node We divide $Q_{0,13}$ by $Q_{0,23}$ in Eqs. (11), (53) and solve for Ω to get

$$\Omega = -\tan^{-1} \left(\frac{\varepsilon_{10}\varepsilon_{30} + \eta_0\varepsilon_{20}}{\varepsilon_{20}\varepsilon_{30} - \eta_0\varepsilon_{10}} \right). \quad (54)$$

Initial true anomaly From Eqs. (7) and (8) we can derive ϑ_0 as follows

$$\vartheta_0 = \sigma_0 - \tan^{-1} \left(\frac{q_2}{q_1} \right). \quad (55)$$

Argument of perigee We divide $Q_{0,31}$ by $Q_{0,32}$ in Eqs. (11), (53) and solve for $\bar{\omega}$, finally we use Eq. (55) to write the relation for ω

$$\omega = -\sigma_0 + \tan^{-1} \left(\frac{q_2}{q_1} \right) + \tan^{-1} \left(\frac{\varepsilon_{10}\varepsilon_{30} - \eta_0\varepsilon_{20}}{\varepsilon_{20}\varepsilon_{30} + \eta_0\varepsilon_{10}} \right). \quad (56)$$

Note that Eqs. (54) and (56) can not be used when the orbit is equatorial ($i = 0$ deg).

APPENDIX C: DERIVATION OF THE VARIATIONAL EQUATIONS OF MOTION

Let us call *first set* $\mathbf{q} = (q_1 \ q_2 \ q_3)^T$ and *second set* $\varepsilon_0 = (\varepsilon_{10} \ \varepsilon_{20} \ \varepsilon_{30})^T, \eta_0$.

First set For the first three variables Eq. (28) is valuated in the orbital frame \mathcal{R} . We manipulate Eqs. (24) - (26) to express \mathbf{q} in function of the components of $\dot{\mathbf{r}}$ in \mathcal{R} . Then, by differentiating \mathbf{q} respect to these components, we get

$$\frac{\partial \mathbf{q}}{\partial \dot{\mathbf{r}}} = \frac{1}{r_0 \omega_0} \begin{bmatrix} \sin \sigma & (1 + q_3/s) \cos \sigma & 0 \\ -\cos \sigma & (1 + q_3/s) \sin \sigma & 0 \\ 0 & -q_3/s & 0 \end{bmatrix}. \quad (57)$$

After plugging Eqs. (36) and (57) into Eq. (28), and calculating the products, the variational equations for q_1, q_2 and q_3 take the form reported in Eqs. (29) - (31).

Second set For the unit quaternion Eq. (28) is valuated in the inertial frame \mathcal{I} . We take the element Q_{11} of the matrix \mathbf{Q} in Eq. (27) and the elements $Q_{0,23}, Q_{0,33}$ of the matrix \mathbf{Q}_0 in Eq. (11), to write

$$\begin{aligned} (1 - 2\varepsilon_{20}^2 - 2\varepsilon_{30}^2) \cos \Delta\sigma + (2\varepsilon_{10}\varepsilon_{20} - 2\eta_0\varepsilon_{30}) \sin \Delta\sigma &= \mathbf{u}_r \cdot \mathbf{i}_X \\ 2\varepsilon_{20}\varepsilon_{30} - 2\eta_0\varepsilon_{10} &= \mathbf{u}_h \cdot \mathbf{i}_Y \\ 1 - 2\varepsilon_{10}^2 - 2\varepsilon_{20}^2 &= \mathbf{u}_h \cdot \mathbf{i}_Z \end{aligned}$$

where \mathbf{u}_r is the direction of \mathbf{r} and $\Delta\sigma = \sigma - \sigma_0$. By differentiating both sides of these equations respect to the components of $\dot{\mathbf{r}}$ in \mathcal{I} and taking into account the relation

$$\frac{d\eta_0}{d\dot{\mathbf{r}}} = -\frac{\varepsilon_{10}}{\eta_0} \frac{d\varepsilon_{10}}{d\dot{\mathbf{r}}} - \frac{\varepsilon_{20}}{\eta_0} \frac{d\varepsilon_{20}}{d\dot{\mathbf{r}}} - \frac{\varepsilon_{30}}{\eta_0} \frac{d\varepsilon_{30}}{d\dot{\mathbf{r}}},$$

derived by differentiating Eq. (16), we get

$$\frac{\partial \varepsilon_0}{\partial \mathbf{r}} = \mathbf{A}^{-1} \mathbf{B} \quad (58)$$

where the elements of the matrices \mathbf{A} and \mathbf{B} are

$$\begin{aligned} A_{11} &= \frac{Q_{0,13}}{\eta_0} \sin \Delta\sigma \\ A_{12} &= -4\varepsilon_{20} \cos \Delta\sigma + \frac{Q_{0,32}}{\eta_0} \sin \Delta\sigma \\ A_{13} &= 4\varepsilon_{30} \cos \Delta\sigma + \frac{Q_{0,11} + Q_{0,22}}{\eta_0} \sin \Delta\sigma \\ A_{21} &= -\frac{Q_{0,22} + Q_{0,33}}{\eta_0} \\ A_{22} &= \frac{Q_{0,21}}{\eta_0} \\ A_{23} &= \frac{Q_{0,13}}{\eta_0} \\ A_{31} &= -4\varepsilon_{10} \\ A_{32} &= -4\varepsilon_{20} \\ A_{33} &= 0, \end{aligned}$$

$$\begin{aligned} B_{11} &= 0 \\ B_{12} &= 0 \\ B_{13} &= 0 \\ B_{21} &= -\frac{Q_{22} \mathbf{i}_z \cdot \mathbf{i}_X}{r_0 \omega_0 s} \\ B_{22} &= -\frac{Q_{22} \mathbf{i}_z \cdot \mathbf{i}_Y}{r_0 \omega_0 s} \\ B_{23} &= -\frac{Q_{22} \mathbf{i}_z \cdot \mathbf{i}_Z}{r_0 \omega_0 s} \\ B_{31} &= -\frac{Q_{32} \mathbf{i}_z \cdot \mathbf{i}_X}{r_0 \omega_0 s} \\ B_{32} &= -\frac{Q_{32} \mathbf{i}_z \cdot \mathbf{i}_Y}{r_0 \omega_0 s} \\ B_{33} &= -\frac{Q_{32} \mathbf{i}_z \cdot \mathbf{i}_Z}{r_0 \omega_0 s}, \end{aligned}$$

and the elements Q_{22} and Q_{32} which appear in \mathbf{B} , according to Eq. (27), take the expressions

$$\begin{aligned} Q_{22} &= (1 - 2\varepsilon_{10}^2 - 2\varepsilon_{30}^2) \cos \Delta\sigma - (2\varepsilon_{10}\varepsilon_{20} + 2\eta_0\varepsilon_{30}) \sin \Delta\sigma \\ Q_{32} &= (2\varepsilon_{20}\varepsilon_{30} + 2\eta_0\varepsilon_{10}) \cos \Delta\sigma - (2\varepsilon_{10}\varepsilon_{30} - 2\eta_0\varepsilon_{20}) \sin \Delta\sigma. \end{aligned}$$

Note that if $\eta_0 = 0$ the matrix \mathbf{A} becomes

$$\mathbf{A} = 2 \begin{bmatrix} \varepsilon_{30} \sin \Delta\sigma & -2\varepsilon_{20} \cos \Delta\sigma & -2\varepsilon_{30} \cos \Delta\sigma + \varepsilon_{10} \sin \Delta\sigma \\ 0 & \varepsilon_{30} & \varepsilon_{20} \\ -2\varepsilon_{10} & -2\varepsilon_{20} & 0 \end{bmatrix}.$$

Eqs. (36) and (58) are employed in Eq. (28) to obtain the variational equations for ε_{10} , ε_{20} , ε_{30} given by Eqs. (32) - (34). Finally, the variational equation for η_0 , reported in Eq. (35), is obtained by differentiating Eq. (16) respect to σ , and then using Eqs. (32) - (34).

REFERENCES

- [1] Peláez, J., Hedo, J. M., and de Andrés, P. R., "A special perturbation method in orbital dynamics," *Celestial Mechanics and Dynamical Astronomy*, Vol. 97, No. 2, 2007, pp. 131–150.
- [2] Hill, G. W., "Researches in the Lunar Theory," *American Journal of Mathematics*, Vol. 1, No. 1, 1878, pp. 5–26.
- [3] Clohessy, W. H., and Wiltshire, R. S., "Terminal Guidance System for Satellite Rendezvous," *Journal of the Aerospace Sciences*, Vol. 27, Sept. 1960, pp. 653–658, 674.
- [4] Lawden, D. F., *Optimal Trajectories for Space Navigation*. London: Butterworth, 1963. Chap. 5.
- [5] Tschauner, J., and Hempel, P., "Rendezvous zu eine in Elliptischer Bahn umlaufenden Ziel," *Astronautica Acta*, Vol. 11, No. 2, 1965, pp. 104–109.
- [6] De Vries, J. P., "Elliptic Elements in Terms of Small Increments of Position and Velocity Components," *AIAA Journal*, Vol. 1, No. 11, 1963, pp. 2626–2629.
- [7] Melton, R. G., "Time-Explicit Representation of Relative Motion Between Elliptical Orbits," *Journal of Guidance, Control, and Dynamics*, Vol. 23, No. 4, 2000, pp. 604–611.
- [8] Yamanaka, K., and Ankersen, F., "New State Transition Matrix for Relative Motion on an Arbitrary Elliptical Orbit," *Journal of Guidance, Control, and Dynamics*, Vol. 25, No. 1, 2002, pp. 60–67.
- [9] Broucke, R. A., "Solution of the Elliptic Rendezvous Problem with the Time as Independent Variable," *Journal of Guidance, Control, and Dynamics*, Vol. 26, July-Aug. 2006, pp. 615–621.
- [10] Bond, V. R., and Allman, M. C., *Modern Astrodynamics: Fundamentals and Perturbation Methods*. Princeton, NJ: Princeton University Press, 1996. P. 151.
- [11] Battin, R. H., *An Introduction to the Mathematics and Methods of Astrodynamics*. Reston, VA: AIAA Education Series, AIAA, revised ed., 1999.
- [12] Hempel, P., and Tschauner, J., "Über Beschleunigungs-programme minimaler Übergangsenergy für das Rendezvous Manöver," *Astronautica Acta*, Vol. 10, No. 3-4, 1964, pp. 221–237.
- [13] Inalhan, G., Tillerson, M., and How, J., "Relative Dynamics and Control of Spacecraft Formations in Eccentric Orbits," *Journal of Guidance, Control and Dynamics*, Vol. 25, No. 1, 2002, pp. 48–59.